J. Jpn. Soc. Soil Phys.
土壌の物理性
No. 159 p.3 ～ 12 (2025)

論　文
Original Paper

Low-cost environmental monitoring technologies: Thermoelectric cooler-based net radiometer and capacitor-resistor oscillation-based soil moisture sensor

Kosuke NOBORIO [1] , Jun-ichi TAZAWA [2], Yuki SHOJI [3], Naoto SHIMOOZONO [3] and Daiki KOBAYASHI [3,**]

Abstract: Using low-cost sensors, the Internet of Things (IoT) on a farm has been popular for monitoring environmental conditions such as temperature, humidity, and CO_2 concentration to evaluate mass and energy balances in the field. However, net radiation and soil moisture sensors are still relatively expensive; thus, low-cost sensors have been required to spread IoT technologies on the farm. In recent years, logic ICs and thermoelectric coolers (TECs) have become readily available at very reasonable prices. Here, we introduced low-cost net radiation and soil moisture sensors. First, a TEC was used to measure net radiation after calibration with a linear regression line. The measurement error was approximately $< \pm 50$ W m^{-2} after eliminating data with the air temperature $<$ the dew point temperature. Then, the capacitor and resistor (CR) oscillator circuit was employed to determine soil water content, assuming soil water as a variable capacitor. After insulating sensing rods, the CR oscillator's output frequency, f, was inversely related to volumetric water contentment, θ. A linear regression line between θ and f yielded a measurement error of $< \pm 0.05$ m^3 m^{-3} with minimal temperature dependence of $d\theta/dT = 0.0006$ m^3 m^{-3} °C^{-1} for 10–40 °C. The data obtained using those sensors would be accurate enough for practical use with IoT.
Key Words : capacitance sensor, salinity effect, Peltier element, dew point temperature, rainfall

1. Introduction

Energy and mass exchanges between atmosphere and ground are among the most essential subjects in soil and environmental sciences, agronomy, engineering, and other disciplines. Recent electronics, sensors, and microcomputer advancements have enabled us to develop inexpensive ecological monitoring systems. For example, Ito et al. (2022) introduced a measuring evapotranspiration system with the Bowen ratio energy balance using an Arduino microcomputer and inexpensive air temperature and humidity sensors. They also used a commercially available net radiometer and a soil heat flux plate, which are expensive.

In previous years, Weaver and Campbell (1985) and Momose and Kasubuchi (2008) successfully used a thermoelectric cooler (TEC) to measure soil heat flux after calibration. Taha et al. (2023) reported a TEC was used to measure solar radiation but not net radiation, which is required to evaluate the surface energy balance. Conventional net radiometers are usually covered with polyethylene domes to reduce natural ventilation and thermal convection from the sensing plate; however, domeless net radiometers are also commercially available, one of which was evaluated by Cobos and Baker (2003) in the field. Recently, the construction of a simple domeless net radiometer using a thermopile was introduced for education purposes by Da Ros Carvalho et al. (2021). Thus, a TEC used as a domeless net radiometer would be worth evaluating for field use because the TEC costs much less than commercially available net radiometers, and there is no need for tedious work to build thermopiles.

Soil moisture sensors other than weather sensors are the most required for soil- (plant-) atmosphere relation studies in the field. The biggest turning year for sensing soil water content may be 1980 when Topp et al. (1980) introduced time-domain reflectometry (TDR) to measure the apparent dielectric constant of soil using electromagnetic (EM) waves. Many review papers on TDR have been published since then, such as Noborio (2001), Robinson et al. (2003), Černý (2009), He et al. (2021), and others. The TDR

[1]School of Agriculture, Meiji University, Kawasaki, Kanagawa 214-8571, Japan. Correspondence: K. Noborio, noboriok@meiji.ac.jp
[2]Formerly School of Agriculture, Meiji University, Kawasaki, Kanagawa 214-8571, Japan.
[3]Formerly Graduate School of Agriculture, Meiji University, Kawasaki, Kanagawa 214-8571, Japan. ** Now at NTT Access Network Service Systems Laboratories,1-7-1 Hanabatake, Tsukuba, Ibaraki, 305-0805, Japan.
2025 年 1 月 3 日受稿　2025 年 2 月 11 日受理

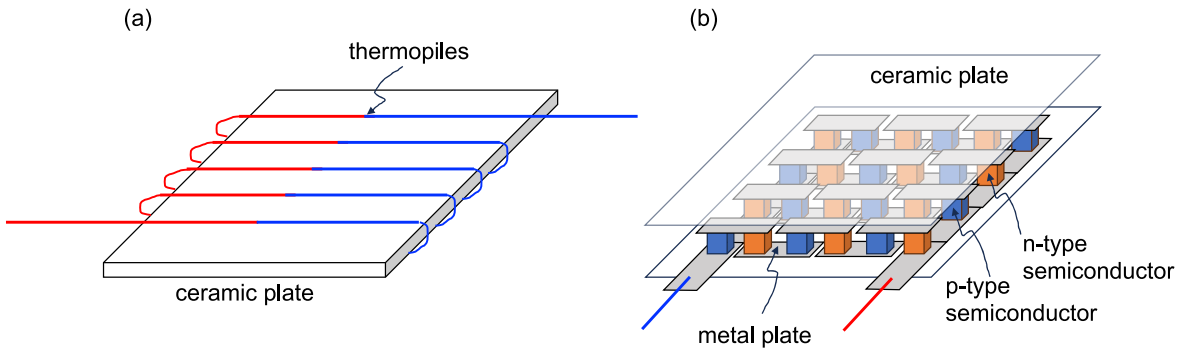

Fig. 1 Schematic diagrams of (a) a conventional net radiometer with thermopiles and (b) a proposed net radiometer with a thermoelectric cooler (TEC).

Photo 1 Net radiometers: TEC (left) and Q*7.1 (right) on top of the rice plants' canopy.

has many advantages over previous methods except one drawback: it requires expensive equipment. After Topp et al. (1980) demonstrated that EM waves could be used to determine soil dielectric constant, other inexpensive techniques using EM waves, such as capacitance sensors by Ruth (1999), Kizito et al. (2008), and Kojima et al. (2016), were introduced for measuring soil moisture. We chose a circuit diagram that Ruth (1999) developed because it was simple enough to build by ourselves yet very inexpensive.

Our objectives for this article were to evaluate a TEC device for measuring net radiation and Ruth's CR oscillator for measuring soil water content as a soil moisture sensor.

2. Materials and Methods

2.1 Net Radiometer

To calibrate a newly developed thermoelectric cooler (TEC) net radiometer and evaluate its real-world performance, we conducted a field experiment in a rice paddy field in central Japan (35° 22' N, 139° 20' E) between the 9th and 19th of September 2008. The TEC device (40 mm long, 40 mm wide, and 4 mm thick, TEC1-12706, Vktech, China) painted with black spray (THI-1B, TASCO JAPAN, Japan) with an emissivity of 0.94 was fixed at the end of polyvinyl chloride (PVC) pipe and installed horizontally at 1.5 m high above the ground in the rice paddy field (Photo 1). In addition, a net radiometer (Q*7.1, Campbell Scientific Inc., Logan, UT) was installed at the same height as the TEC. Net radiation was measured at 10-second intervals and averaged every 5 minutes using a data logger (CR23X, Campbell Scientific Inc., Logan, UT). Net radiation measured for the first two days with the Q*7.1 was used to calibrate the TEC. The voltage output of the TEC device was calibrated with the Q*7.1 measured net radiation converted from the Q*7.1 voltage output using the coefficient provided by the manufacturer. In addition, environmental conditions, including precipitation, air temperature, and relative humidity, were measured at 1.5 m high above the ground and the wind speed at 2 m high every 5 min to investigate those effects on measurement using the TEC.

Conventional net radiometers use thermopiles to generate electric current through the Seebeck effect, which depends on temperature differences between the upper and lower surfaces (Fig. 1a). Our proposed new net radiometer utilizes the TEC to create electric current based on the same principle as thermopiles; however, the TEC features n-type and p-type semiconductors, as shown in Fig. 1b. Many TEC devices are used in computers to cool CPUs, making them widely available at much lower prices than thermopiles, which are often harder to find in markets.

2.2 Soil Moisture Sensor

A capacitance soil moisture sensor was developed based on the CR oscillation circuit using SN74 ICs presented by Ruth (1999) (Fig. 2). Since SN74 ICs are widely distributed for logic circuits, they are readily available. The capacitance soil moisture sensor treats soil as a combination of a capacitor, C, and a resistor, R. The oscillation frequency, f, changes depending on the values of C and R. The oscillation frequency, f (Hz), may be calculated as

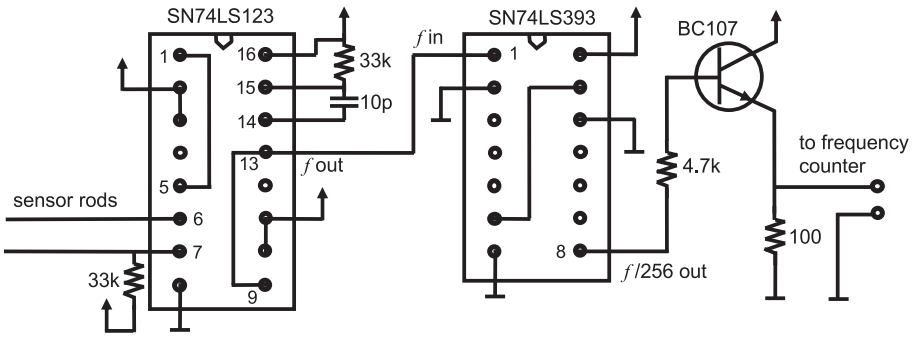

Fig. 2 Schematic diagram of a soil moisture sensor (modified from Ruth, 1999).

(Maier, 2020):

$$f = \frac{dc}{t_w} \approx \frac{dc}{RC} \quad (1)$$

where dc is the duty cycle in fraction, t_w is the output pulse duration (s), R is the resistance (Ω), and C is the capacitance (F). The value of C is expressed as a function of soil moisture content, i.e., relative permittivity, ε, and the value of R as a function of soil moisture and salinity; therefore, changes in soil moisture content are interpreted as changes in oscillation frequency.

An SN74LS123 holds two units of a monostable multivibrator in it. The C of 10 pF and R of 33 kΩ connected to pins 14 to 16 of SN74LS123 made a trigger with the output pulse duration, t_w, and output at pin 13 as $f$out from the 1st unit of monostable multivibrator. Part of the $f$out signal was sent to pin 9 to trigger the 2nd unit of the monostable multivibrator, which added frequency shift due to capacitance changes resulting from soil moisture changes at pin 6 and pin 7 connecting to sensor rods. The output signal from the 2nd unit at pin 5 was directly sent to pin 1 as a trigger signal for the 1st unit. As $f$in, part of the $f$out signal at pin 13 was sent to pin 1 of a frequency divider made of SN74LS393, a four-stage binary counter. The output signal at pin 8 of SN74LS393 was one 256th of $f$in frequency. The $f$out from pin 8 was connected to a frequency counter through a switching transistor, BC107.

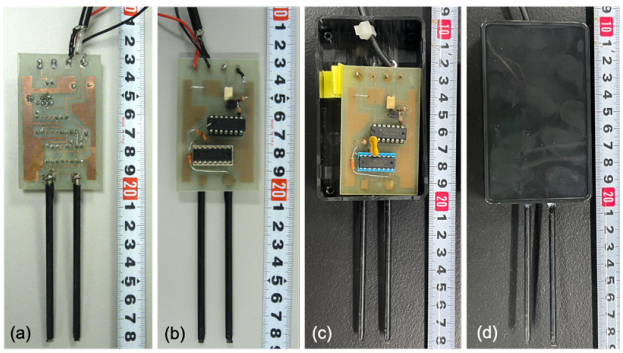

Photo 2 A soil moisture sensor on the PCB: (a) etched copper side, (b) electronic components side, (c) the PCB placed in a plastic box (100 × 60 × 25 mm), and (d) the PCB placed in a plastic box with a lid closed.

For the first soil-moisture sensor, the required electronic components were arranged and connected on a universal circuit board. For its sensing probe, two stainless steel bare rods, 1.6 mm in diameter and 74 mm long, were fixed in parallel using the epoxy resin 15 mm apart. The two stainless-steel rods were connected to the CR oscillation circuit via a 50 Ω coaxial cable approximately 1.2 m long. The distance between the sensing rods and the oscillation circuit should have been short since the output frequency fluctuated when hands touched the coaxial cable. A frequency counter (MXG-9802X, METEX, Korea) was used to measure the oscillation frequency, which varied with soil moisture content and salinity.

The first soil moisture sensor with bare rods was assessed for basic performance and subsequently tested using Toyoura sand. The probe was also submerged in various concentrations of NaCl solution to examine the effects of salinity. Later, the rods were encased in insulated tubes and tested in NaCl solutions and Toyoura sand with various water contents.

To avoid output frequency fluctuation by touching the coaxial cable, we built the second soil moisture sensor on a printed circuit board (PCB) using the same circuit diagram shown in Fig. 2. The PCB sensor did not have a coaxial cable to connect the circuit board to rods but directly connected stainless-steel rods (3.2 mm diameter, 80 mm long, and 15 mm apart) to the circuit board (Photos 2a, b). Rods with a diameter of 3.2 mm enhanced the sensor's rigidity, preventing wobbling and altering the output frequency. The stainless-steel rods were insulated by covering them with heat-shrinkable tubes made of polyolefin resin, which made the rods' diameters 3.8 mm, following Nadler and Lapid (1996). The PCB sensor was placed in a plastic box (100 × 60 × 25 mm) to protect the sensor circuit from dust and water (Photos 2c, d). Output frequency was measured with an oscilloscope (SDS1102, OWON Technology

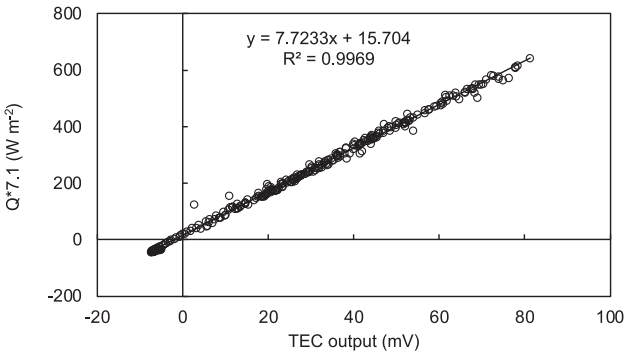

Fig. 3 The output voltage of the TEC was linearly calibrated to net radiation, R_n, measured with the Q*7.1 net radiometer when air temperature > dew point temperature, meaning no dew condensed on the TEC surfaces.

Inc., China) or a frequency counter (KIT-10140, SparkFun Electronics, U.S.A.).

After air-dried, 2 mm sieved Toyoura sand (100 % sand and 0 % clay) and Kanto loam (40 % sand and 15 % clay) were separately mixed with distilled water to different moisture contents, i.e., volumetric water contents varying from 0.002 to 0.34 $m^3\ m^{-3}$ for Toyoura sand and from 0.107 to 0.43 $m^3\ m^{-3}$ for Kanto loam, in sealed plastic bags and mixed thoroughly. The mixed soil remained undisturbed for an hour, and then the soil was packed in a cylindrical container (inner dia. = 5.0 cm, height = 10.2 cm) to constant bulk densities ($\approx$ 1.44 Mg m^{-3} and 0.79 Mg m^{-3} for Toyoura sand and Kanto loam, respectively). The sensing rods were vertically inserted into the packed soil from the soil surface, and the output frequency was measured. The soil was then oven-dried to determine the water content. All the experiments were conducted in a laboratory at room temperature, around 25 °C.

Lastly, the PCB sensor with the insulated rods, inserted in an air-dried Toyoura sand packed in a cylindrical container (inner dia. = 5.0 cm, height = 10.2 cm), was placed in a constant temperature chamber between 10 and 40 °C. The air-dried Toyoura sand was used for this purpose since it is reported that air-dried soils have the most significant temperature effects on the output from a frequency domain reflectometry (Noborio and Kubo, 2017). The soil surface was covered with a thin plastic film to reduce soil water content changes in Toyoura sand.

3. Results and Discussion

3.1 Net Radiometer

3.1.1 Calibration

Since air temperature and relative humidity were measured, dew point temperature was determined. When air temperature was lower than dew point temperature, dew might be condensed on the TEC surface. Thus, the TEC device was calibrated with the Q*7.1 net radiometer using data collected between September 9 and 11, excluding those with air temperature < dew point temperature. A significant linear relationship ($p < 0.001$) was found between output voltage from the TEC device and net radiation, R_n, measured with the Q*7.1 net radiometer (Fig. 3). Even with some outliers, the TEC output voltage responded linearly to R_n, ranging between -40 and 610 W m^{-2}. There was an intercept in the linear regression equation, meaning that $R_n = 0$ did not show up simultaneously in both net radiometers. This could be due to the two net radiometers not being perfectly leveled or the differing emissivity of the plant canopy beneath both net radiometers.

3.1.2 Field measurement

Temporal changes in precipitation and net radiation, R_n, measured with the Q*7.1 and the TEC device, were compared in Fig. 4. The two devices measured slight differences in R_n during the daytime, especially after the September 16 and 18 rain events. There was no delay in the TEC device responding to R_n changes, even sudden changes. During the midday of sunny September 12–14 days, the TEC device provided higher R_n than the Q*7.1. In contrast, after the September 16 and 18 rain events, the TEC device provided much lower R_n than the Q*7.1 during the daytime. Even though there was ample precipitation during nighttime on September 16, there was not much difference in R_n between the two devices. Water droplets formed on the TEC surface reduced R_n values only during the daytime.

Although most data were closely scattered around the 1 : 1 line, part of the data measured with the TEC was lined up with a smaller gradient than the 1 : 1 line (Fig. 5a). As suspected in the clear morning (Cobos and Baker, 2003) or after rainfall events, condensed dews or water droplets on the TEC surfaces might deviate from the TEC data from the 1 : 1 line. By eliminating the TEC data when the air temperature was lower than the dew point temperature, the small gradient part disappeared in Fig. 5b, as expected. The slope of the regression line between net radiation, R_n, measured with Q*7.1 and the TEC, was very close to unity. The TEC performed well when there were no dews or water droplets on the surfaces, meaning that using the TEC device was limited when the air temperature was higher than the dew point temperature. This limitation, however, would be similar to a commercial domeless net radiometer (Cobos and Baker, 2003).

3.1.3 Measuring errors

Since we noticed subtle differences between the Q*7.1 and TEC devices, temporal changes in those differences

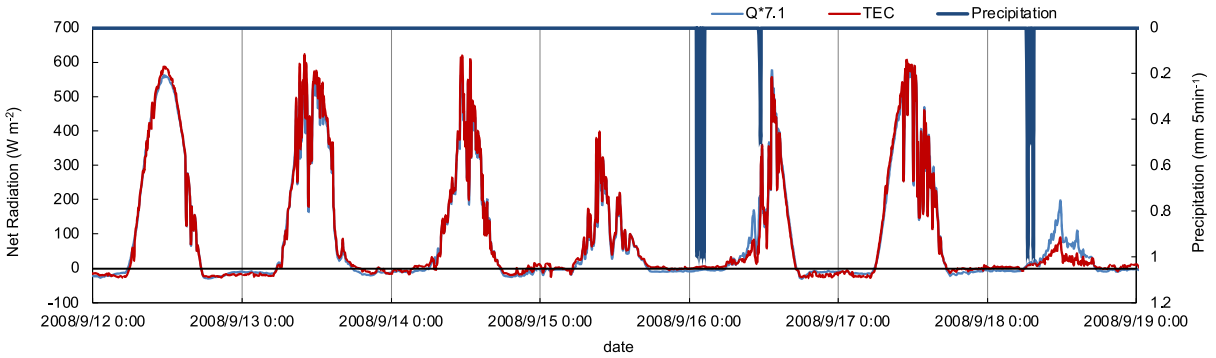

Fig. 4 Temporal changes in precipitation and net radiation, R_n, measured with the Q*7.1 net radiometer and the TEC device, were compared.

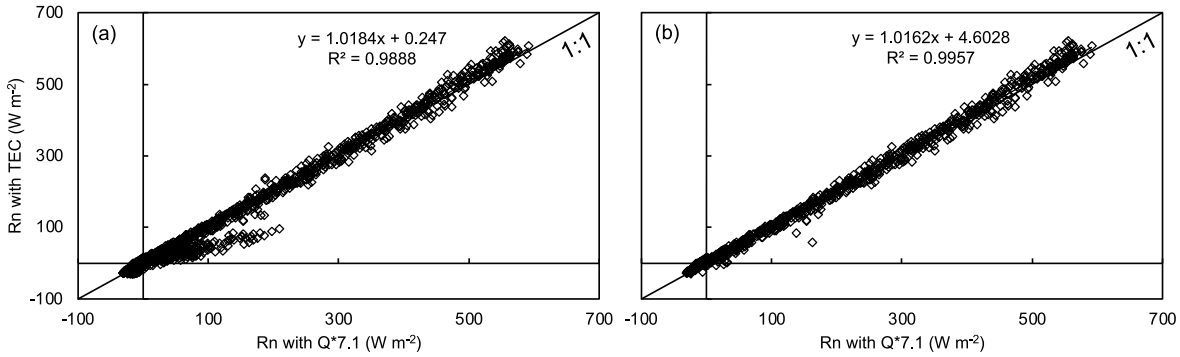

Fig. 5 The relationship of net radiation, R_n, measured with Q*7.1 and the TEC device: (a) with all the data, and (b) with only the data of air temperature > dew point temperature.

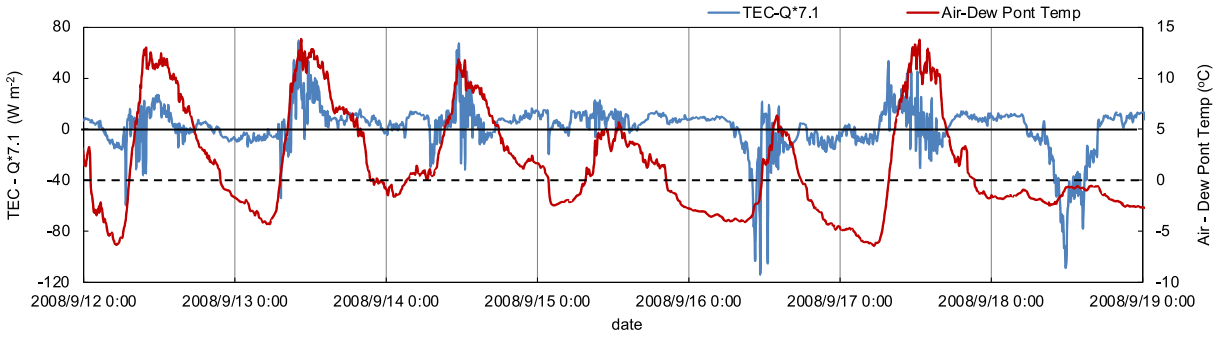

Fig. 6 Temporal changes in R_n difference, TEC - Q*7.1, and temperature difference, air-dew point. When air temperature < dew point temperature, meaning negative temperature differences, dew might be condensed on the TEC surfaces.

and dew formation timing were illustrated in Fig. 6. We assumed that dew was formed when air temperature < dew point temperature. Dew was formed between late night and morning on sunny days, September 12 and 13. When the dew was formed, TEC measured R_n to be smaller than R_n measured by Q*7.1, which showed negative values in Fig. 6. Latent heat loss due to vaporizing dew decreased the TEC's up-faced surface temperature, especially after sunrise; thus, TEC measured R_n became smaller than Q*7.1. On the rainy days of September 16 and 18, raindrops on the TEC's up-faced surface made the up-faced surface temperature cooler than the down-faced surface.

During midday on sunny September 12-14 days, R_n measured with the TEC gradually became higher late morning than those with the Q*7.1, and the highest around noon, then became smaller early afternoon. There was no such phenomenon in the overcast sky during midday on September 15. This was supposed to be that the sun's shortwave irradiance heated the TEC's up-faced surface. Differences in R_n measured with both net radiometers dur-

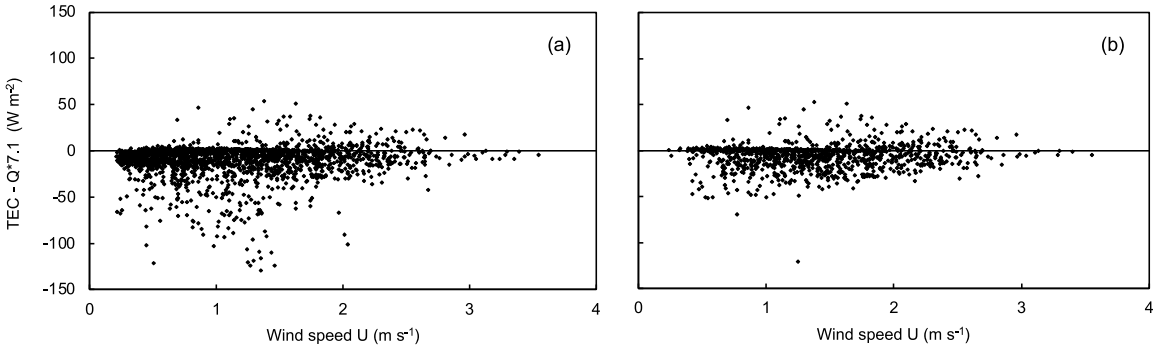

Fig. 7 Measurement errors of R_n depending on wind speed: (a) all the data, and (b) data without when air temperature < dew point temperature.

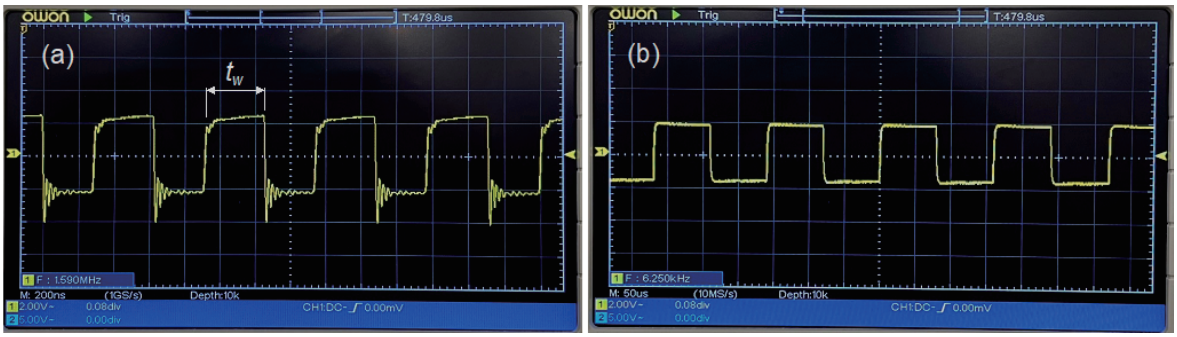

Photo 3 Screenshots of the oscilloscope: (a) the oscillator output at pin 1 of SN74LS123, and (b) the output to a frequency counter at pin 8 of SN74LS393. Insulated rods with the PCB sensor were placed in the air.

ing midday might result from black paints with different emissivity on the surfaces of the net radiometers.

The difference in R_n measured between Q*7.1 and the TEC varied with wind speed (Fig. 7). The difference was relatively large for wind speeds ranging between 0.5 and 2 m s^{-1}. With all the data, R_n with the TEC was underestimated over 100 W m^{-2} due to the cooling effect of evaporating dews and water droplets when the wind speed < 2 m s^{-1} (Fig. 7a). For the data with the air temperature $>$ the dew point temperature, the measurement difference became small (Fig. 7b), approximately $< \pm 50$W m^{-2}, compatible with the measurement errors of a commercial domeless net radiometer (Cobos and Baker, 2003). Although Cobos and Baker (2003) recommended the wind speed correction for > 5 m s^{-1}, that may not be necessary for our data because all the data measured at < 3.5 m s^{-1} (Fig. 7).

Although the performance of a TEC net radiometer was comparable to that of a commercially available model, a significant drawback is that TEC net radiometers typically last only 3 to 4 years, or even less, due to circuit failures. The internal circuitry of a TEC consists of a series of n-type and p-type semiconductors, as demonstrated in Fig. 1b; thus, if just one semiconductor fails, it leads to total failure.

3.2 Soil Moisture Sensor

3.2.1 Oscillator and frequency divider

After the insulated rods were placed in the air and the PCB sensor was turned on by being supplied with 6 VDC, SN74LS123 started oscillation. The C of 10 pF and R of 33 kΩ connected to pin numbers 14 to 16 of SN74LS123 made a trigger signal with the output pulse duration, t_w, of approximately 330 ns, well compared to the measured value of 335 ns with approximate 50 % duty cycle as shown in Photo 3a. The oscillation frequency, f, was 1.59 MHz measured at pin 1 of SN74LS12, well compared to the theoretical values as in Eq. 1, and the output frequency of square waves was 6.25 kHz measured at pin 8 of SN74LS393 (Photo 3b), which was approximately $1/256$ of 1.59 MHz. When the insulated rods were immersed in the distilled water, the output frequency was 3.97 kHz, i.e., the oscillation frequency $f = 1.02$ MHz. Such a frequency range between 1 MHz and 1 GHz is suitable for soil moisture measurement because the dielectric constant, ε, does not strongly depend on the frequency (Topp et al., 1980) and soil type (Černý, 2009).

The output frequencies in the air and water ranged between 6.25 kHz and 3.97 kHz, respectively. This range corresponded to ε between 1 and 80 for the air and water (Noborio, 2001). Since soil water contents between air-dry

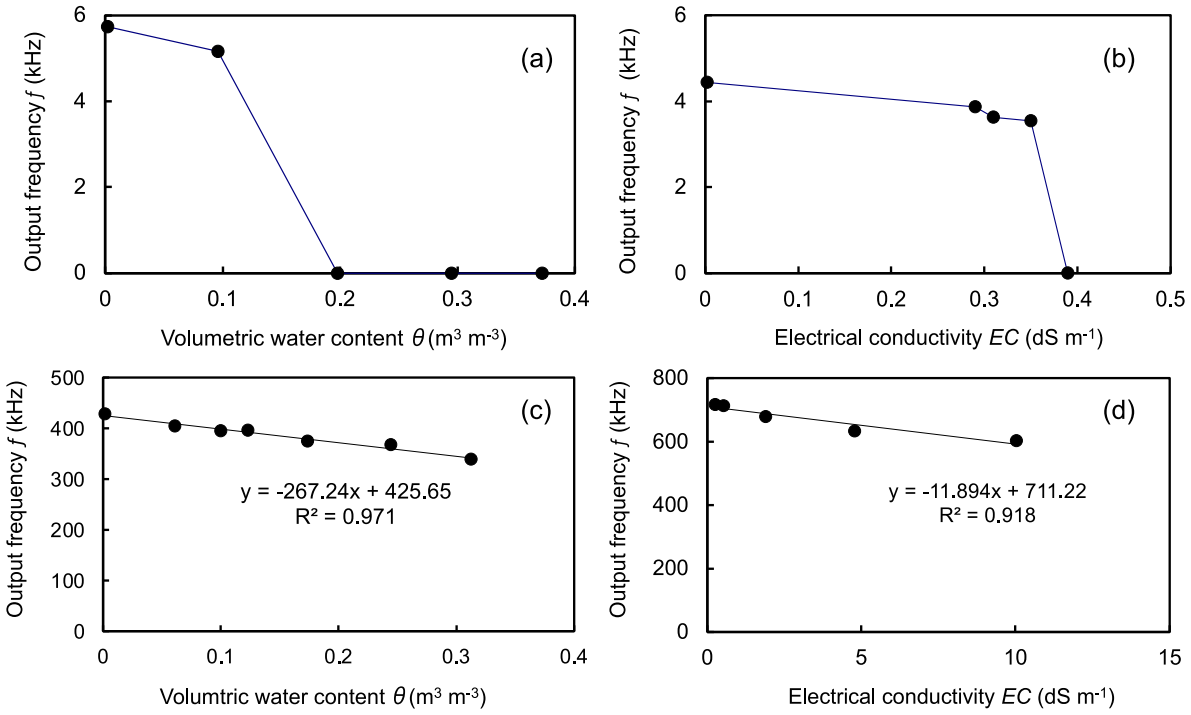

Fig. 8 Changes in frequency measured with bare stainless-steel rods of the first soil moisture sensor in Toyoura sand (a) and in NaCl solution (b), and those with insulated rods in Toyoura sand (c) and in NaCl solution (d).

and saturation usually range between $\varepsilon = 3$ and 40 (Topp et al., 1980), our PCB sensor could detect changes in soil water contents as the output frequencies ranged between 6.21 kHz and 5.13 kHz if ε and f are linearly related.

3.2.2 Bare rods

When the bare stainless-steel rods connected to the first soil moisture sensor were used as a sensing probe, oscillation stopped in Toyoura sand with $\theta > 0.1$ m^3 m^{-3} (Fig. 8a) and in NaCl solution with $EC > 0.35$ dS m^{-1} (Fig. 8b). Since soil water contains some electrolytes, increased soil water content reduces the soil's electrical resistance, resulting in a short circuit between the bare rods to stop oscillation. Similarly, in the NaCl solution, increasing EC made a short circuit between the bare rods to prevent oscillation. Our soil moisture sensor was much more prone to salinity than TDR, whose bare-rods probe is reported to be short-circuited in NaCl solutions with $EC > 126$ dS m^{-1} or concentration > 0.1 mol kg^{-1} (Noborio, 2001).

3.2.3 Insulated rods

When the insulated stainless-steel rods connected to the first soil moisture sensor were used as a sensing probe, a short circuit did not interrupt the oscillation in varying water contents of Toyoura sand (Fig. 8c) and several concentrations of NaCl solution (Fig. 8d). The output frequency, f, was linearly correlated with the volumetric water content, θ, and EC (Figs 8c, d). While insulating the rods made the sensor less susceptible to salinity than uncoated rods, utilizing TDR remains beneficial in saline soil. These findings indicate that the rods should be insulated to measure even non-saline soils' water content.

Using the insulated rods for the PCB sensor, output frequency, f, changed according to various water contents between air-dry and near saturation. As volumetric water content, θ, increased, f decreased for both soils (Fig. 9a). Kanto loam had a slightly higher output f than Toyoura sand for similar water contents. The output frequency, f, and volumetric water content, θ, for Toyoura sand and Kanto loam had a significant linear relationship ($r = 0.943$, $n = 14$, $p < 0.001$). The measured values were mainly scattered within ± 0.05 m^3 m^{-3} around the regression line, as indicated by dashed lines in Fig. 9a. Unlike the ε-θ relationship used for TDR calibration, the f-θ relationship for the capacitance soil moisture sensor was linear. Furthermore, there was little difference in f-θ relationships between Toyoura sand and Kanto loam, a volcanic ash origin having a unique ε-θ relationship (Miyamoto et al., 2001). These characteristics of the capacitance sensor we introduced would be suitable for practical use in field experiments. For more precise measurements required, a calibration for an individual soil was performed: $y = -5.2208x + 5.9317$, $r = 0.995$ for Toyoura sand, and $y = -4.4259x + 6.1110$, $r = 0.992$ for Kanto loam.

3.2.4 Temperature effect

Although the dielectric constant of water has a slight temperature dependency, temperature has little effect on TDR measured θ (Topp et al., 1980). Capacitance

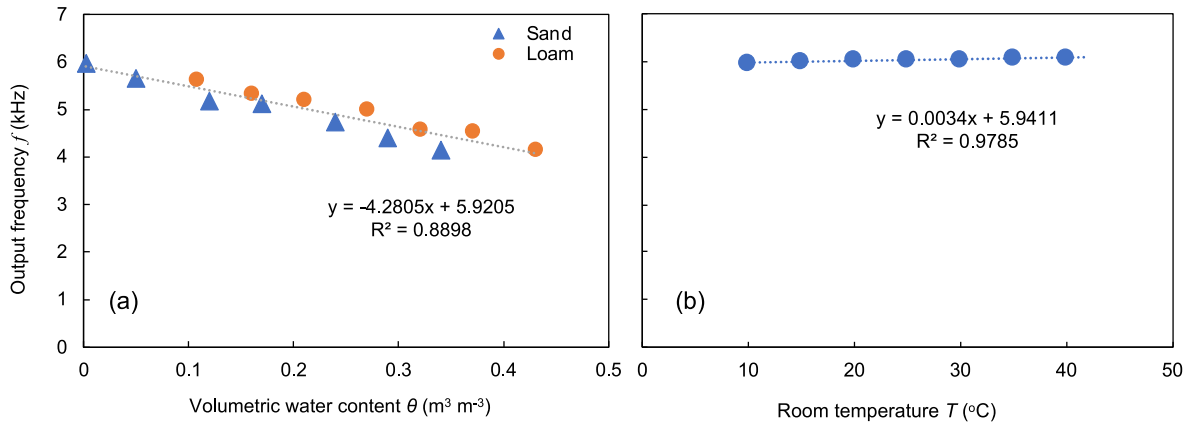

Fig. 9 Changes in frequency measured with the PCB sensor: (a) in Toyoura sand and Kanto loam with various θs, and (b) in air-dried Toyoura sand at various room temperatures between 10 and 40 °C. The solid line indicates a regression line, the dashed lines indicate $\theta \pm 0.05$ m^3 m^{-3} in (a), and the dotted line indicates a regression line in (b).

probes, in contrast, are generally recognized as slightly temperature-dependent on θ measurements (Noborio and Kubo, 2017). For air-dried Toyoura sand, output frequency slightly increased as room temperature increased from 10 to 40 °C (Fig. 9b). Changes in frequency against room temperature were significantly linear with $r = 0.989$, $n = 7$, $p < 0.001$. The largest output frequency increase was 0.1 kHz, equivalent to $\theta = 0.018$ m^3 m^{-3} decrease when the room temperature changed from 10 to 40 °C. The temperature dependency, $d\theta/dT$, was then determined as 0.0006 m^3 m^{-3} °C^{-1}, which was about 2.5 times as less temperature dependency as one reported for a commercial soil moisture sensor with 0.0015 m^3 m^{-3} °C^{-1} (Noborio and Kubo, 2017). The temperature effect probably occurred because of the oscillator's C and R temperature dependencies. As temperature increases, the *R*-value increases, decreasing oscillation frequency, which contradicts the measurement. As temperature rises, on the other hand, the *C*-value decreases, increasing oscillation frequency. It is assumed that increases in the oscillator's *C*-value increased the oscillation frequency as room temperature rose, and increased *R*-value with decreased *C*-value compensated each other; thus,the temperature dependency of the sensor became small enough for practical use.

4. Conclusions

This study introduced and evaluated two low-cost environmental monitoring technologies: a thermoelectric cooler (TEC)-based net radiometer and a capacitor-resistor (CR) oscillator-based soil moisture sensor. Our findings demonstrate that these cost-effective alternatives can provide sufficient accuracy for practical applications in agriculture and environmental monitoring.

(1) Net radiometer performance
  (a) The TEC device, calibrated against a commercial net radiometer using a linear regression model, exhibited strong agreement in net radiation measurements.
  (b) Measurement accuracy was within ±50 W m^{-2}, provided that data collected when the air temperature was below the dew point were excluded.
  (c) The TEC device performed comparably to commercial domeless net radiometers, offering a low-cost alternative for field energy balance studies.
  (d) However, dew formation and wind speed variations introduced minor measurement errors, which should be considered in field applications.

(2) Soil moisture sensor performance
  (a) The CR oscillator-based capacitance sensor initially failed in moist conditions due to short-circuiting of the bare stainless-steel rods. However, this issue was resolved by insulating the rods, leading to a stable and linear relationship between oscillation frequency (f) and volumetric water content (θ).
  (b) Measurement accuracy was within ±0.05 m^3 m^{-3}, making the sensor suitable for practical soil water content monitoring.
  (c) The sensor demonstrated minimal temperature dependency ($d\theta/dT = 0.0006$ m^3 m^{-3} °C^{-1}), significantly better than commercial capacitance-based soil moisture sensors.
  (d) Unlike time-domain reflectometry (TDR), which is more resilient to salinity, the capacitance sensor with bare stainless-steel rods remains susceptible to high electrical conductivity ($EC > 0.35$ dS m^{-1}), highlighting the need for further optimization in saline soils.

(3) Final remarks

The TEC-based net radiometer and CR oscillator-based soil moisture sensor provide affordable and effective alternatives to commercial environmental monitoring systems. While dew formation, wind speed effects, and salinity sensitivity pose challenges, the overall performance of these low-cost sensors makes them highly suitable for IoT-driven agricultural and environmental applications. Future work should explore further calibration, long-term stability, and potential adaptations to enhance sensor durability and measurement reliability.

Acknowledgments

We thank Uizin Co., Ltd. in Tokyo for their assistance in developing the first soil moisture sensor.

References

Černý, R. (2009): Time-domain reflectometry method and its application for measuring moisture content in porous materials: A review. Measurement, 42(3): 329–336, doi:10.1016/j.measurement.2008.08.011.

Cobos, D.R., Baker, J.M. (2003): Evaluation and modification of a domeless net radiometer. Agron. J., 95(1): 177–183, doi:10.2134/agronj2003.1770.

Da Ros Carvalho, H., McInnes, K.J. and Heilman, J.L. (2021): Construction of a simple domeless net radiometer for demonstrating energy balance concepts in a laboratory activity. Atmosphere, 12(12): 1620, doi:10.3390/atmos12121620.

He, H., Aogu, K., Li, M., Xu, J., Sheng, W., Jones, S.B., González-Teruel, J.D., Robinson, D.A., Horton, R., Bristow, K., Dyck, M., Filipovic', V., Noborio, K., Wu, Q., Jin, H., Feng, H., Si, B. and Lv, J. (2021): A review of time domain reflectometry (TDR) applications in porous media. In: Sparks, D.L. (Ed.), Advances in Agronomy, 168. Academic Press, pp. 83–155, doi:10.1016/bs.agron.2021.02.003.

Ito, Y., Hirashima, Y., Miyamoto, H. and Momii, K. (2022): Application of Arduino and CMOS temperature-humidity sensor to evapotranspiration calculation by Bowen ratio energy budget method. J. Jpn. Soc. Soil Phys., 150: 115–123, doi:10.34467/jssoilphysics.150.0_115. (in Japanese with English abstract)

Kizito, F., Campbell, C.S., Campbell, G.S., Cobos, D.R., Teare, B.L., Carter, B. and Hopmans, J.W. (2008): Frequency, electrical conductivity and temperature analysis of a low-cost capacitance soil moisture sensor. J. Hydrol., 352(3–4): 367–378, doi:10.1016/J.JHYDROL.2008.01.021.

Kojima, Y., Shigeta, R., Miyamoto, N., Shirahama, Y., Nishioka, K., Mizoguchi, M. and Kawahara, Y. (2016): Low-cost soil moisture profile probe using thin-film capacitors and a capacitive touch sensor. Sensors, 16(8): 1292, doi:10.3390/s16081292.

Maier, E. (2020): Designing with the SN74LVC1G123 monostable multivibrator. Application Report. Texas Instruments Inc.

Miyamoto, T., Kobayashi, R., Annaka, T. and Chikushi, J. (2001): Applicability of multiple length TDR probes to measure water distributions in an Andisol under different tillage systems in Japan. Soil and Till. Res., 60(1–2): 91–99, doi:10.1016/S0167-1987(01)00172-6.

Momose, T. and Kasubuchi, T. (2008): Measurement of soil heat flux using a thermos-module. J. Jpn. Soc. Soil Phys., 108: 91–98, doi:10.34467/jssoilphysics.108.0_91. (in Japanese with English abstract)

Nadler, A. and Lapid, Y. (1996): An improved capacitance sensor for in situ monitoring of soil moisture. Soil Res., 34(3): 361–368, doi:10.1071/SR9960361.

Noborio, K. (2001): Measurement of soil water content and electrical conductivity by time domain reflectometry: a review. Comput. Electr. Agric., 31(3): 213–237, doi:10.1016/S0168-1699(00)00184-8.

Noborio, K. and Kubo, T. (2017): Evaluating a dual-frequency-phase-shift soil moisture and electrical conductivity sensor. PAWE., 15: 573–579, doi:10.1007/s10333-016-0574-7.

Robinson, D.A., Jones, S.B., Wraith, J.M., Or, D. and Friedman, S.P. (2003): A review of advances in dielectric and electrical conductivity measurement in soils using time domain reflectometry. Vadose Zone J., 2(4): 444–475, doi:10.2113/2.4.444.

Ruth, B. (1999): A capacitance sensor with planar sensitivity for monitoring soil water content. Soil Sci. Soc. Am. J., 63: 48–54, doi:10.2136/sssaj1999.03615995006300010008x.

Taha, M., Omar, M., Khan, S., Usman, M., Larkin, S. and Imran, M. (2023): A Low-cost IoT-enabled pyranometer; based on the Peltier element. International Journal of Engineering Trends and Technology, 71(2): 334–340, doi:10.14445/22315381/IJETT-V71I2P235.

Topp, G.C., Davis, J.L. and Annan, A.P. (1980): Electromagnetic determination of soil water content: Measurements in coaxial transmission lines. Water Resour. Res., 16(3): 574–582, doi:10.1029/WR016i003p00574.

Weaver, H.L. and Campbell, G.S. (1985): Use of Peltier coolers as soil heat flux transducers. Soil Sci. Soc. Am. J., 49(4): 1065–1067, doi:10.2136/sssaj1985.03615995004900040054x.

要　　旨

廉価センサーを用いた農地における IoT 技術は，温度，湿度，CO_2 濃度などの環境条件をモニタリングし，圃場での物質およびエネルギー収支を評価するために広く利用されている．しかし，正味放射量センサーや土壌水分センサーは依然として比較的高価であり，IoT 技術を農地に普及させるためには廉価なセンサーが求められている．近年，論理 IC やペルチェ素子（TEC）が非常に手頃な価格で容易に入手可能となっている．本研究では，低コストの正味放射量センサーおよび土壌水分センサーを製作した．まず，TEC を用いて正味放射量を測定し，線形回帰直線による較正を行った．気温が露点温度未満の場合のデータを除去した後，測定誤差はおよそ ± 50 W m^{-2} 未満であった．次に，コンデンサ · 抵抗（CR）発振回路を用いて土壌水分量を測定した．土壌水分を可変容量コンデンサとして仮定すると，センサー棒を絶縁した後，CR 発振回路の出力周波数 f は体積含水率 θ に反比例する関係を示した．θ と f の間の線形回帰直線に基づく測定誤差は ± 0.05 m^3 m^{-3} 未満であり，温度依存性は 10–40 °C の範囲で $d\theta/dT = 0.0006$ m^{3}m^{-3}°C^{-1} と小さかった．これらのセンサーを用いて得られたデータは，IoT での実用に十分な精度を有すると考えられる．

キーワード：静電容量センサ，塩分の影響，ペルチェ素子，露点温度，降雨